Secondary sonic boom propagation through stratified atmosphere with 3-D wind

S. L. Chernyshev and L. G. Ivanteyeva
Central Aerohydrodynamic Institute named after prof. N.E. Zhukovsky (TsAGI)
1 Zhukovsky Street, Zhukovsky, Moscow region 140180, Russia

Abstract
Propagation of secondary sonic boom generated by maneuvering airplane in stratified atmosphere with 3-D wind is investigated. Conditions for secondary boom occurrence and ray reflection altitude are derived. According to the reflection altitude the secondary boom rays are classified as stratospheric and thermospheric ones. Influence of every wind velocity component and airplane heading on secondary sonic boom exposure zones is demonstrated. Peculiarities of signal passage through the singular turnaround point are discussed. Calculations of secondary boom signatures show essential influence of airplane acceleration and atmospheric parameter gradients along flight trajectory on the shock wave intensity and its shape.

1. Introduction

Supersonic airplane environment impact study should not disregard secondary sonic booms, representing shock waves arriving to the ground after reflection in the upper atmosphere. In the paper conditions for secondary boom appearance are cosidered. These conditions represent simple relations between stratified atmosphere parameters and airplane flight regime. It has been shown that the ray turnaround condition has very helpful graphical interpretation that allow to define whether secondary boom occurs or not. Sonic boom exposure zones are considered at the realistic atmosphere state and different airplane headings. Peculiarities of signal passage through the singular turnaround point, where the ray tube area cut by horizontal plane has singular ambiguity are discussed. Analysis of secondary boom propagation through stratified atmosphere from maneuvering airplane has revealed considerable influence of atmospheric and flight regime factors on both shock wave intensity and its shape.

2. Conditions for ray to turn around and secondary sonic boom to occur

In the terms of geometric acoustics, equations for the ray path in stratified atmosphere may be reduced to invariant[1,2,3] that depends on vector $\mathbf{V}_{gr}$ of airplane velocity relative to the ground[4] as follows:

$$\frac{\mathbf{n}'}{a+\mathbf{v}\cdot\mathbf{n}} = const = \frac{\mathbf{n}'_0}{a_0+\mathbf{v}_0\cdot\mathbf{n}_0} = \frac{\mathbf{n}'_0}{a_0+\left(\mathbf{V}_{gr}-\mathbf{V}_0\right)\cdot\mathbf{n}_0} = \frac{\mathbf{n}'_0}{\mathbf{V}_{gr}\cdot\mathbf{n}_0}\,. \tag{1}$$

Here $\mathbf{n}$ is the unit vector normal to the wavefront, $\mathbf{n}'$ is the horizontal component of $\mathbf{n}$, a is the speed of sound, $\mathbf{v}$ is the vector of wind velocity, and $\mathbf{V_0}$ is the vector of airplane velocity relative to air particles on the flight trajectory. Index «0» refers to the parameters at the ray origin. Relation (1) after simple transformation may be rewritten at turnaround point as:

$$\left(\mathbf{V}_{gr}-\boldsymbol{\eta}\right)\cdot\mathbf{n}_0 = 0\,, \tag{2}$$

where $\boldsymbol{\eta}$ is, so called, the vector of state function with magnitude equaled to $\eta = (a^2 - v_y^2)^{1/2}+U$ and direction along $\mathbf{n'_0}$ (we name this direction below as the ray azimuth), U and v_y are components of wind velocity along the ray azimuth and vertical axis y, respectively. Condition (2) means equality of projections onto $\mathbf{n_0}$ of the airplane velocity and disturbance velocity at turnaround point. It should be noted that horizontal component of wind velocity, which is perpendicular to the ray azimuth, does not curve the ray path and condition (2) does not depend on it. Relation $(\mathbf{V_{gr}} - \boldsymbol{\eta})\cdot\mathbf{n}_0 > 0$ is valid along the ray with nonzero path slope to horizon. Let $\boldsymbol{\eta}^-_{max}$ be maximum value of $\boldsymbol{\eta}$-function along the ray azimuth below the airplane and $\boldsymbol{\eta}^+$ be the value of $\boldsymbol{\eta}$-function at turnaround point above it. The first condition for the ray to reach the ground level is

$$(\mathbf{V}_{gr} - \boldsymbol{\eta}^{-}_{\max})\cdot\mathbf{n}_0 > 0. \tag{3}$$

The vector $\boldsymbol{\eta}^{+}$ satisfies relation (2). Taking into account that vector $\boldsymbol{\eta}^{-}_{\max}$ is parallel to vector $\boldsymbol{\eta}^{+}$, the second condition for the secondary boom ray reflection in the upper atmosphere is:

$$\boldsymbol{\eta}^{+} \geq \boldsymbol{\eta}^{-}_{\max}. \tag{4}$$

Equality sign in (4) corresponds to boundary azimuths for secondary sonic booms propagation. Relation (4) defines azimuth range, in which appearance of secondary sonic booms is possible. We name it as atmospheric condition. Relations (3) and (4) represent separately necessary conditions and together - sufficient conditions for secondary boom appearance.

3. Geometrical interpretation of secondary boom propagation azimuths

Condition (2) defines the only value $\boldsymbol{\eta}$ for the ray reflections in atmospheric layers both below and above the airplane. Hence, the altitudes for the ray to turn around may be easily obtained for the selected ray azimuth. In order to idetify specific rays we name by "thermospheric ray" or "stratospheric ray" respective rays in accordance with the layer of their reflection. Without loss of generality, we assume that the upper atmosphere reflects the whole fan of disturbances. Local temperature maximum is available in stratosphere at the altitude of approximately 50 km with the value closed to the temperature maximum below the airplane. Specific airplane regimes and atmospheric states may cause rays to turn around in the stratosphere and reach the ground. These stratospheric disturbances are of prime importance because of their larger intensity.

A. *Level flight*. Azimuth ranges coincide for secondary sonic boom rays directed initially downward and upward. Geometrical interpretation of the condition (2) in this case is shown in Fig. 1*a*: the projection $\mathbf{V}_{gr}$ onto the ray azimuth equals $\boldsymbol{\eta}$ at turnaround point. Let us denote angle between the vectors $\mathbf{V}_{gr}$ and $\boldsymbol{\eta}$ as ν. Angles ν on both sides from the vector $\mathbf{V}_{gr}$ are different if vectors $\mathbf{V}_{gr}$ and horizontal component of wind velocity $\mathbf{v'}$ at turnaround level are non-collinear. The picture is symmetrical with respect to the vector $\mathbf{V} = \mathbf{V}_{gr} - \mathbf{v'}$. Inside of the azimuth range ν the ray passes through the layer with non-zero angle to horizon. The ray never reaches this layer if its azimuth is outside ν range. Analysis of azimutal ranges for stratospheric secondary booms is rather simple if two levels with two maximum values $\boldsymbol{\eta}^{-}_{\max}$ below the airplane and $\boldsymbol{\eta}^{+}_{\max}$ in the stratosphere are known. Applying Fig. 1*a*, first of all, for $\boldsymbol{\eta}^{-}_{\max}$ level, one may obtain azimuth range for secondary/primary sonic booms. Atmospheric parameters of the $\boldsymbol{\eta}^{+}_{\max}$ level define two boundary azimuths between stratospheric and thermospheric rays (dashed lines). It is evident that if these boundaries do not belong to the azimuth range of secondary sonic booms defined before stratospheric secondary boom does not occur.

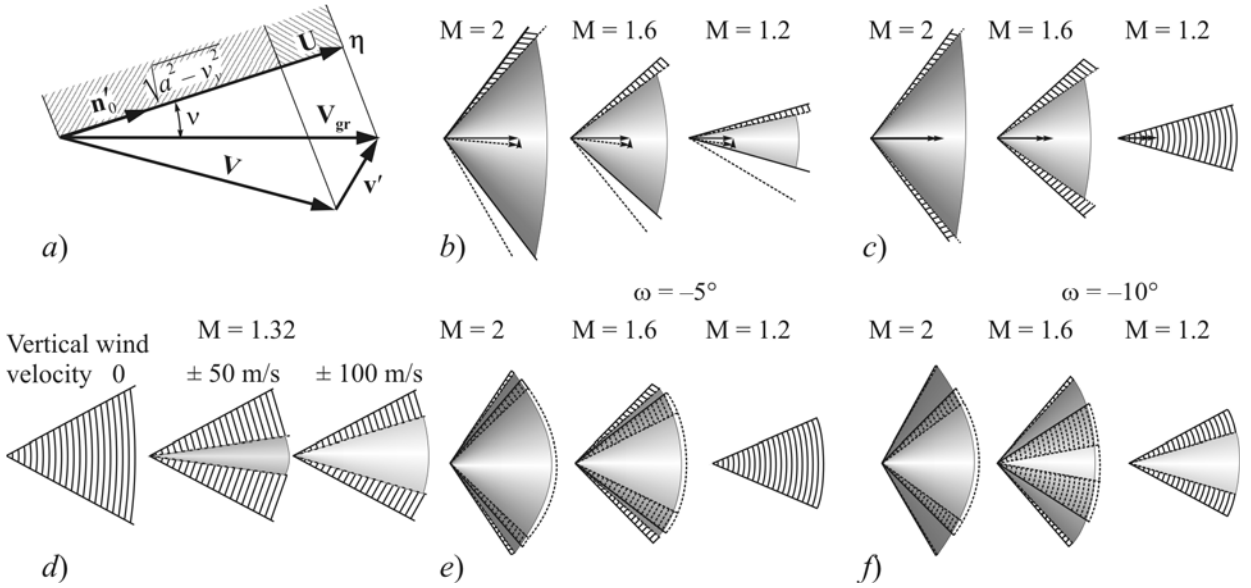

Figure 1: *a*) Geometrical interpretation of the condition for the ray to turn around: *a* is sound speed, $\mathbf{V}_{gr}$ is the airplane velocity, $\mathbf{v'}$ and v_y are horizontal and vertical components of the wind velocity; azimuth ranges for secondary sonic booms propagation in various samples of stratospheric wind: *b*) cross wind; *c)* favourable wind ; *d*) 3-D wind; *e*) – *f*) flight along trajectory with angle ω to horizon in atmosphere with favourable wind

To observe evolution of azimuth ranges of secondary booms for various atmosphere and flight conditions, we consider standard atmosphere with various stratospheric winds: *b*) cross wind, *c*) favourable horizontal wind, and *d*) favourable wind in the presence of vertical wind (Fig. 1*b–d*, respectively). Horizontal wind reaches its maximal value of 60 m/s at the beginning of stratopause. In Fig. 1*b–f* continuous filling refers to thermospheric boom ranges and solid line hatch refers to stratospheric ones. Qualitative analysis for *b*) and *c*) cases at M = 2 was considered earlier[5]. Cross wind causes radial shift of thermospheric azimuth range and enlarges the range itself. These effects result in narrowing of stratospheric ranges as Mach number decreases. Favourable wind strengthens atmospheric reflecting ability. Stratospheric azimuth range becomes larger as the airplane decelerates. The whole reflection in the stratosphere occurs first when the disturbance velocity coincides with $\mathbf{V}_{gr}$ and lasts until the airplane velocity reaches the value $\boldsymbol{\eta}^{-}_{\max}$. Atmospheric condition (4) fails for oncoming wind and for the rays on the right track side if cross wind blows. Therefore, stratospheric booms cannot appear in these cases. Influence of 3-D wind consists of independent contributions of its horizontal $\mathbf{v}'$ and vertical v_y velocity components. Fig. 1*d* illustrates comparative influence of these components. The coupling moment of stratospheric azimuth ranges is selected for favourable wind case. Presence of vertical wind results in a gap between stratospheric ranges. The more the value $|v_y|$ is, the more rays penetrate into layers of thermosphere. To compensate influence of favourable wind of 60m/s, vertical wind must reach the value of ~ 190 m/s.

B. *Non-level flight.* Fig. 1*e* and Fig. 1*f* show azimuth ranges for the airplane flying in atmosphere with favourable wind along trajectory with angle ω to horizon equaled to –5º and –10º. For non-level trajectory azimuth ranges are different for rays initially downward and upward. Stratospheric azimuth ranges for these rays are marked by solid and dash hatch, respectively. Trajectory inclination results in undesirable extension of the total stratospheric azimuth ranges. Geometric interpretation may be applied in this case also by introducing equivalent level velocity $\mathbf{V}_{eq}$ for every ray azimuth. In accordance with (1), the value of $\mathbf{V}_{eq}$ is defined from the relation: $\mathbf{V}_{gr}\cdot\, \mathbf{n}_0 = \mathbf{V}_{eq}\cdot\, \mathbf{n}'_0$.

4. Sonic booms carpets from manoeuvring airplane

Sonic boom carpets for unsteady flight regimes in realistic atmosphere with horizontal wind are considered below. Atmospheric parameters are presented in Fig. 2. As shown above, the main factor defining whether stratospheric sonic booms occur or not is wind strength and its direction with respect to the airplane heading. Let β_{at} be the angle between *x*-axis and some certain azimuth direction (clockwise direction is positive). Condition (4) results in approximately 135° azimuth range for possible stratospheric booms, namely: $-35° \leq \beta_{at} \leq 100°$. Boundary stratospheric azimuths will be marked further by dotted line. Such range estimation is rather exact although it does not include horizontal shift of the ray trajectory away from the ray azimuth plane.

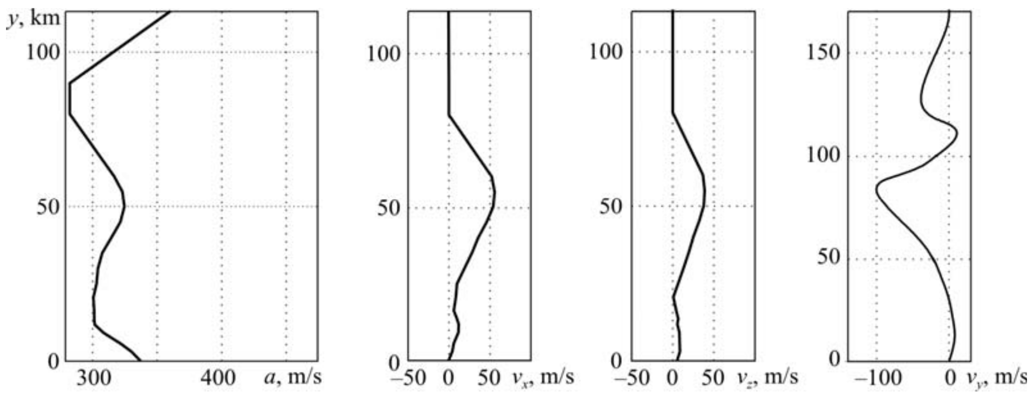

Figure 2: Atmospheric parameters: *a* – sound speed;
v_x – east–west(+), v_z – south–north(+), and v_y – vertical wind velocity components

A. *Flight with descent and deceleration.* Airplane starts decent and deceleration from the altitude of 17 km. Mach number, descent rate, and airplane acceleration are: 2.0, –10 m/s, and –1/3 m/s^2, respectively. We denote airplane heading as the angle β between the airplane velocity azimuth and axis *x* (Fig. 3*a*). Its range is –105° ÷ 175° with step of 35° (Fig. 3*b–k*). Lines of sonic booms ground reflection are shown for disturbances emitted in 100 seconds time interval. Black colour marks primary sonic boom locations; purple and blue colours refer to secondary sonic booms emitted initially upward and downward, respectively. We assume linear growth of sound speed along the altitude in thermosphere until the occurrence of whole reflection. So, the ray propagation in the thermosphere may be considered only as qualitative one. Stratospheric secondary sonic boom rays do not occur for β = – 105º and 175º

(Fig. 3*b*,*k*). Headings –70º and 140º (Fig. 3*c*,*j*) allow rays penetrate into the range of possible stratospheric directions. Nearly cross wind blows in the stratosphere for these cases, so we observe evolution of azimuth ranges analogous to that considered above in Fig. 1*b*: narrow azimuth ranges decrease and vanish at all as the airplane decelerates. Stratospheric booms fall to the ground from one side of the airplane track if headings almost coincide with atmospheric boundary azimuths (β = –35º and 105º, Fig. 3*d*,*h*). For β = 0º and 70º (Fig. 3*e*,*g*) stratospheric carpets are located from both sides of the track transforming to the symmetrical view as the airplane heading tends to the prevailed stratospheric wind direction (β = 35º, Fig. 3*f*).

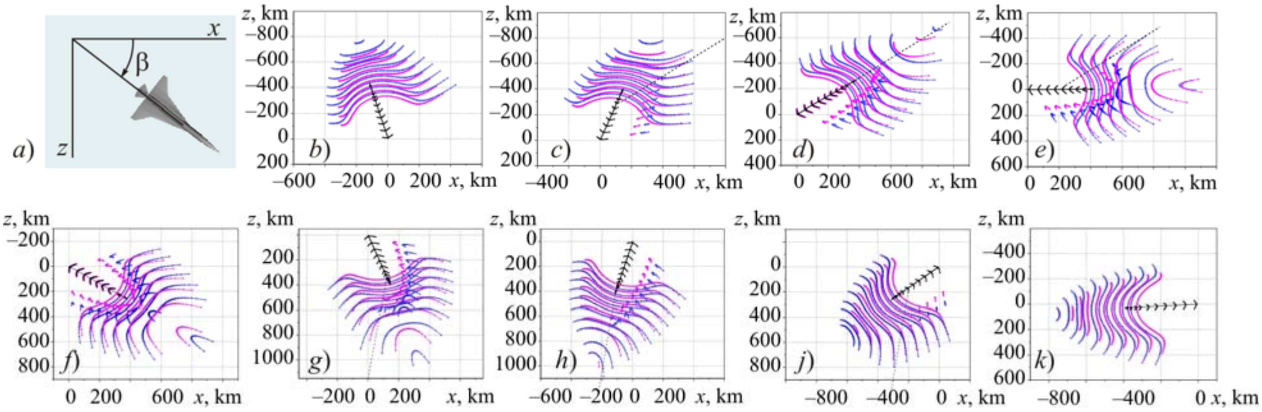

Figure 3: Sonic booms ground reflections

B. *Climbing flight with acceleration.* Evolution of sonic boom carpets for two climbing flights with acceleration are shown in Fig. 4: g_x = 1/3 m/s^2 (left side of the figure) and g_x = 2/3 m/s^2 (right side of the figure). Starting conditions are similar: the airplane flies at the altitude of 9 km (above the coordinate system origin) at M = 1.05. Accelerations and rates of climb V_y are selected in such a way to achieve the altitude of 17 km at Mach number 2.0. Lines of sonic booms ground reflection are shown for the rays emitted in 20 seconds along the flight trajectory and are marked as above in Fig. 3. Concentration of this line is the indicator of sonic boom strengthening. For every type of sonic boom carpets, regions exist where disturbances fall twice. So, an observer may receive sonic boom, for instance, 5 times (primary boom plus 4 thermospheric booms), 6 times (4 thermospheric booms plus 2 stratospheric booms initially downward or upward). Taking into account repeated stratospheric reflections, the number of registered booms might be increased.

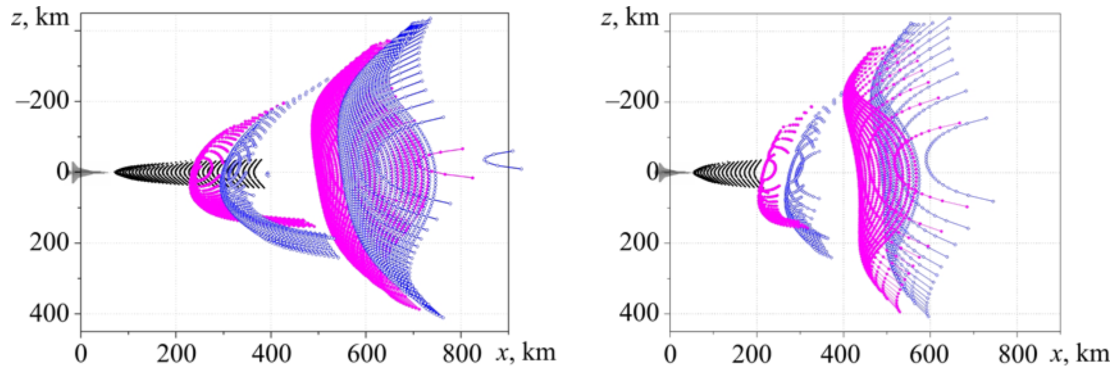

Figure 4: Sonic booms carpets for the airplane accelerated climbing flight (left panel: g_x = 1/3 m/s^2, V_y = 10 m/s and right panel: g_x = 2/3 m/s^2 , V_y = 19.6 m/s)

5. Disturbance propagation in the atmosphere with vertical wind

Vertical wind is rather weak in atmosphere below the airplane[5]. So its influence on primary sonic booms is not significant. Unlike this, secondary sonic boom disturbances pass twice through the atmospheric layers with vertical wind, which value may achieve 100 m/s. Let us consider realistic vertical wind share shown in Fig. 2. Three specific features of the ray path in the atmosphere with vertical wind may be revealed. Two first features refer to the level flight: the ray path does not depend, first, on vertical wind velocity at the emission level and, second, on vertical wind direction for definite azimuth. The third one states that the ray path is symmetrical with respect to the vertical line drawn through the turnaround point. As the example, Fig. 5*a* illustrates thermospheric rays emitted in the airplane symmetry plane in the atmosphere without vertical wind and with vertical winds of opposite directions. Ray emission altitude is 15 km and Mach number equals 2.0. Ray paths coincide for opposite vertical winds and this path can hardly be distinguished from the ray path in the atmosphere without vertical wind. The question arises, in what the influence of vertical wind appears. The fact is that the ray propagates along the same path but with different velocities in the atmosphere with opposite vertical winds. Fig. 5*b* shows different time of the ray arrivals at concrete altitude for considered samples of atmosphere. Another picture takes place for flights with descent/ascent. Slope of flight trajectory splits turnaround level for definite ray azimuth in the atmosphere with opposite vertical winds. Positive vertical wind at the ray origin increases turnaround altitude for both initially upward and downward rays. For instance, Fig. 5*c* illustrates how alteration of vertical wind direction forces thermospheric ray to become stratospheric one for descending flight with $V_y = -10$ m/s.

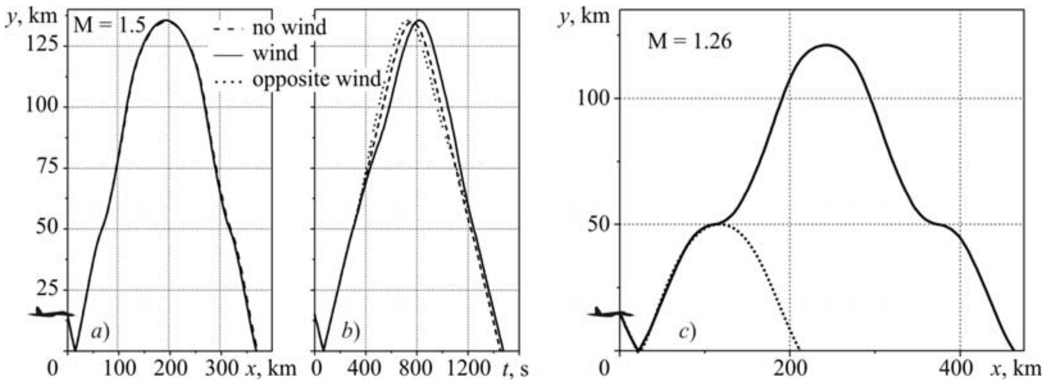

Figure 5: *a*) Ray paths for three samples of vertical winds; *b*) time for the ray passage through concrete altitude; *c*) the ray paths for non-level flight in the atmosphere with opposite vertical winds

6. Disturbance passage through the singular turnaround point

Ray propagates through the turnaround point with zero inclination angle to the horizon. It was shown earlier[6] that calculation of primary sonic boom intensity along the grazing ray is associated with algorithmic difficulties when passing through the turnaround point because of mathematical singularity. That is why restriction on the ray-path slope[3] (~ 0.07º) was introduced. Analogous problem must be overcome for the every secondary sonic boom ray, which by definition turns around in the upper atmosphere. We discuss below the extension of the approach[6] to the secondary boom propagation in stratified atmosphere with horizontal wind.

To define sonic boom signature, two variables k and k_1, which depend on the ray tube area cut by horizontal plane in explicit form, must be calculated. The value of this area is proportional to a product $n_y I(y)$. Proportionallity coefficient is constant along the ray. Function $I(y)$ represents algebraic combination of three integrals as: $I(y) = (1-\sigma^2)I_1(y) + \sigma^2 I_2(y) + 2\sigma(1-\sigma^2)^{1/2} I_3(y) - \gamma/a_0[I_1(y)I_2(y) - I_3^2(y)]$. These integrals and parameters γ and σ are given below:

$$I_1(y) = a_0 \int_H^y \left[\frac{a}{a_*} + \frac{a(\mathbf{I}_0 \Delta\mathbf{v})^2}{n_y^2 a_*^3} \right] \frac{dy}{n_y}, \qquad I_2(y) = a_0^3 \int_H^y \frac{a}{n_y^2 a_*^3} \frac{dy}{n_y}, \qquad I_3(y) = a_0^2 \int_H^y \frac{a(\mathbf{I}_0 \Delta\mathbf{v})}{n_y^2 a_*^3} \frac{dy}{n_y},$$
$$\gamma = \frac{n_{0y}^2 \operatorname{tg}^2 \mu}{a_0^2 (1 - \cos^2 \omega \sin^2 \theta)} \left[\mathbf{g} \cdot \mathbf{n_0} - \frac{a_0 \sin^2 \omega}{n_{0y} \sin^2 \mu} \left(\frac{da_0}{dh} + \mathbf{n_0} \cdot \frac{d\mathbf{v_0}}{dh} \right) \right], \tag{5}$$
$$\sigma = \frac{\cos\mu \sin\omega + \sin\mu \cos\omega \cos\theta}{|\cos\mu \sin\omega + \sin\mu \cos\omega \cos\theta|} \frac{n_{0y}}{\sqrt{1 - n_{0y}^2}} \frac{\cos\omega \sin\theta}{\sqrt{1 - \cos^2 \omega \sin^2 \theta}},$$

here the vector $\mathbf{l}_0$ lies in horizontal plane $y = const$ and is tangent to wave front surface, $\Delta\mathbf{v} = \mathbf{v} - \mathbf{v}_0$, $a_* = a_0 - \Delta\mathbf{v}\cdot\mathbf{n}_0$, H is the altitude of the ray origin, $\mathbf{g}$ is the vector of airplane acceleration, $\mu = \sin^{-1}(1/M)$, $\omega = \sin^{-1}(V_y|\mathbf{V}_0|)$, θ is cylindrical angle around the vector of airplane velocity $\mathbf{V}_0$ relative to air particles on the flight trajectory. To simplify formulas, we introduce relative value of the ray tube area ε as $\varepsilon = n_y I(y)$. At the turnaround point, this value represents singular ambiguity of 0·∞ type. To reveal this ambiguity, we substitute the integration variable n_y for y in formulas (5). Differentiation of the relation $n_y^2 = 1 - n^2$ results in: $n_y dn_y = -c(y)dy$. Formulas for variables k, k_1, and $c(y)$ are:

$$k \sim \int_H^{\hat{y}} \frac{1}{a^2\sqrt{a\rho|\varepsilon(y)|}}\frac{dy}{n_y}, \quad k_1 \sim \left[\frac{\hat{a}^3\hat{\rho}}{\varepsilon(\hat{y})}\right]^{1/2}, \quad c(y) = n_0'^2 \frac{a}{a_*}\frac{d}{dy}\frac{a}{a_*} = \frac{n'^2}{a}\left(\frac{da}{dy} + \frac{dU}{dy}n'\right), \quad c(\hat{y}) = \frac{1}{\hat{a}}\frac{d\eta}{dy}. \tag{6}$$

Superscripts «∩» refer to quantities evaluated at turnaround point. Substitution transforms integrals (5) to the following view:

$$I_i = \int_{n_y}^{n_{0y}} \frac{f_i(n_y)dn_y}{n_y^2} \;(i = 1, 2, 3), \quad f_1 = a_0\left[n_y^2 + \frac{(\mathbf{l}_0\Delta\mathbf{v})^2}{a_*^2}\right]\frac{a}{ca_*}, \quad f_2 = a_0^3 \frac{a}{ca_*^3}, \quad f_3 = a_0^2 \frac{a(\mathbf{l}_0\Delta\mathbf{v})}{ca_*^3}. \tag{7}$$

Let us assume that functions $f_i(n_y)$ may be presented as Taylor's series in the neighborhood of turnaround point. Restricting by two first terms of series and taking into account that $f_i'(0) = 0$, one may write the exact relations:

$$I_i = \frac{\hat{f}_i}{n_y} + A_i; \qquad A_i = \int_{n_y}^{n_{0y}} \frac{f_i(n_y) - \hat{f}_i}{n_y^2} dn_y - \frac{\hat{f}_i}{n_{oy}}, \tag{8}$$

Integrand expressions in (8) are terminal at turnaround point and equal $f_i''(0)/2$. Calculation of $f_i(0)$ and $f_i''(0)$ may be done beforehand because relation (2) uniquely defines the altitude for the ray reflection. Expression to define $\varepsilon(\hat{y})$ may be written as:

$$\varepsilon_{n_y \to \pm 0} = a_0 \frac{a}{ca_*^3}\left\{\left[a_0\sigma + \sqrt{1-\sigma^2}(\mathbf{l}_0\Delta\mathbf{v})\right]^2 - \frac{\gamma}{a_0}\left[a_0^2 A_1 + A_2(\mathbf{l}_0\Delta\mathbf{v})^2 - 2a_0 A_3(\mathbf{l}_0\Delta\mathbf{v})\right]\right\}\Bigg|_{y=\hat{y}}. \tag{9}$$

Thus, every singular integral (7) may be represenred as the sum of continuous integral function along the ray path and first order pole singularity. Fig. 6 (left panel) illustrates example for asimptotic behaviour of I_1, I_2, I_3 integrals and ray tube area ε depending on n_y in a neighborhood of turnaround point. Dependence of the ray tube area on time for different values of the airplane acceleration is examplified in Fig. 7 on the right panel. Realization of considered algorithm fails in two cases. Firstly, ray propagates infinitely long if $d\eta/dy = 0$ at reflection level and, secondly, variable k has unremovable singularity if focussing (ε = 0) occurs at turnaround point under the condition $d\varepsilon/dn_y = 0$.

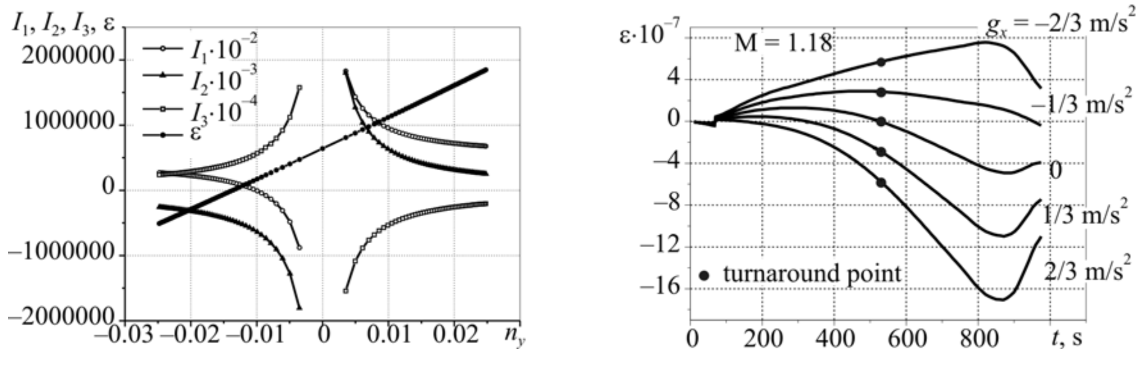

Figure 6: Singular integrals I_1, I_2, I_3, and ray tube area ε in the vicinity of turnaround point (left panel). Dependence of the ray tube area on time for different values of the airplane acceleration (right panel)

7. Features of secondary boom wave propagation

In order to filter out the maneuvering effect, we consider atmospheric parameters shown in Fig. 2 with modification $d\eta/dy = const$ in reflecting layers of the stratosphere. Airplane starts descent from the altitude of 17 km, at M = 2, with descent velocity $V_y = -10$ m/s, heading $\beta = 0$, and different values of horizontal acceleration $g_x = 0$, ±1/3, ±2/3 m/s^2.. Parameter γ is the only factor to define influence of acceleration on the ray tube area and, hence, sonic boom signature. Fig. 7*a* shows the ray tube area distribution along the line of booms ground reflection depending on original ray path slope to horizon $\delta_0 = \tan^{-1}(n_{0y}/n'_0)$ for initially upwards rays. The influence of the atmospheric gradients at the ray origin is equivalent to that of acceleration. As one may see in Fig. 7*b*, increase of both descent rate and acceleration results in analogous effects in considered case.

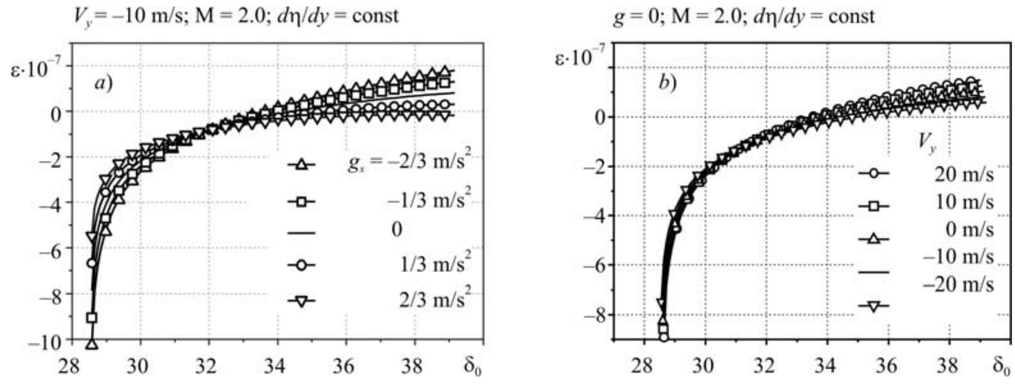

Figure 7: Dependence of the ray tube area ε on the initial ray path angle to horizon δ_0 for different values of the airplane: *a*) acceleration and *b*) vertical velocity V_y

Let us consider now initially downwards rays from the airplane flying at M = 1.18, altitude $H = 10300$ m with descent rate $V_y = -10$ m/s. Fig. 8*a* shows the line of ground reflection. Fig. 8*b* represents the ray tube area distribution in lateral direction for 5 selected values of accelerations. On its way back to the ground, ray may touch caustic surface once, twice, and do not touch it at all. Flight with deceleration –1/3 m/s^2 is the most unfavourable one for considered sample of atmosphere. Airplane maneuvering affects secondary boom intensity in non-predictable way, for instance, for the ray ($\theta = 0$) deceleration –1/3 m/s^2 strengthens intensity and acceleration 2/3 m/s^2 weakens it. Fig. 6 (right panel) shown above illustrates evolution of ε in time along this ray for different values of acceleration.

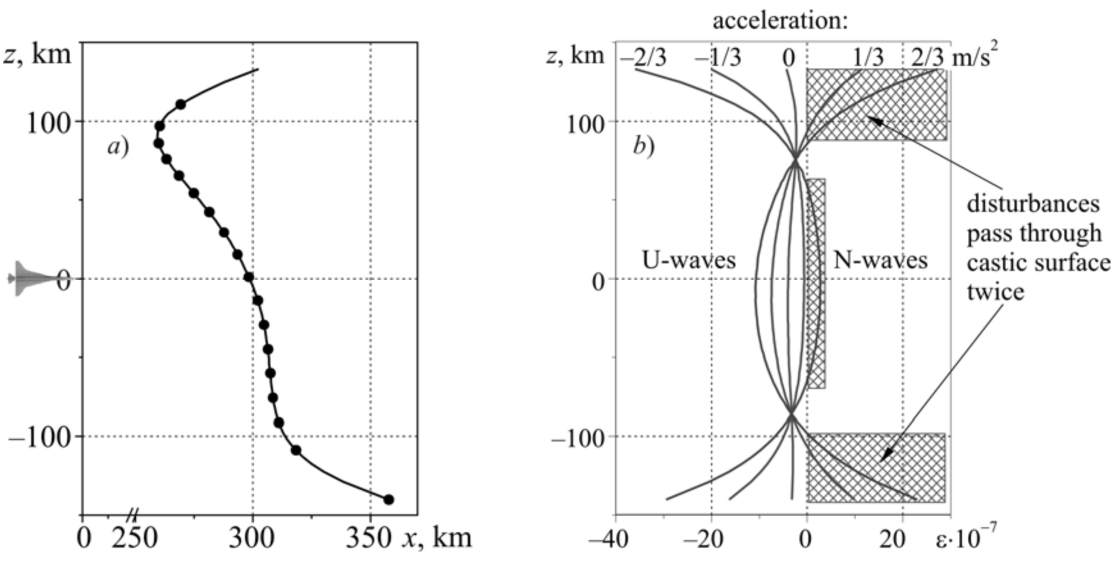

Figure 8: *a*) Line of boom ground intersection and *b*) ray tube area distribution along this line for different flight accelerations at rays' emission time

Sonic boom signatures for this ray are presented in Fig. 9 for *a*) near field and different airplane accelerations: *b*) $g_x = -2/3$ m/s^2, *c*) –1/3 m/s^2, *d*) 0, *e*) 1/3 m/s^2, and *f*) 2/3 m/s^2. Approach[7] as a phase advance of $\pi/2$ for the wave spectrum has been considered for the ray passage through a caustic surface. Overpressure is singular in the vicinity of caustic for such approach; nevertheless, we assume that this solution is correct enough far away from a caustic surface to make estimations under consideration. Account for nitrogen and oxygen molecular relaxation[8] has been considered too. Preliminary results show that waveform and its intensity essentially depend on the value of the airplane acceleration: for $g_x = -2/3$ m/s^2 N-type wave falls to the ground; as far as the value of acceleration increases ($g_x = -1/3$ m/s^2) the waveform transforms into U-type, and for $g_x = 2/3$ m/s^2 waveform tends to accept N- type form again.

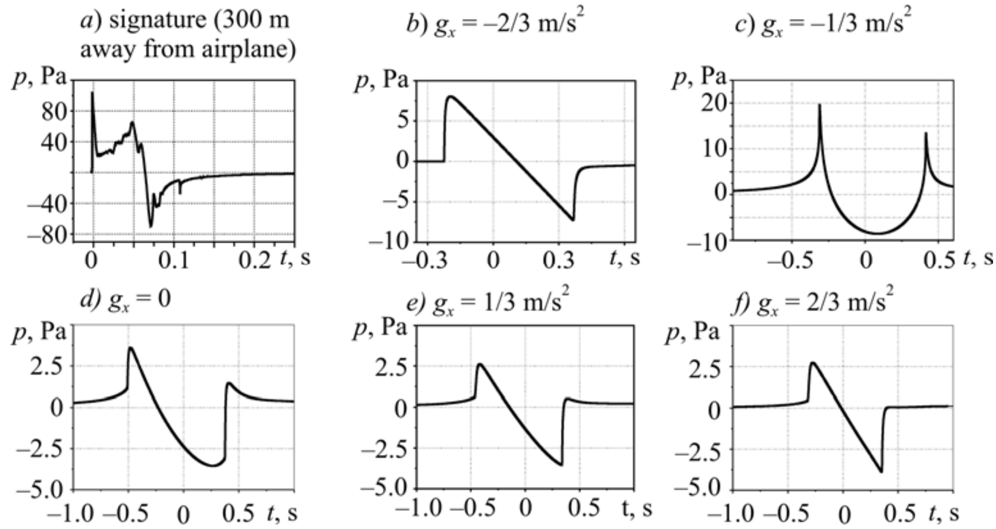

Figure 9: Signatures for *a*) near field and *b*) – *f*) different values of airplane acceleration g_x

Conclusions

Some perculiarities of secondary sonic boom propagation through stratified atmosphere with 3-D wind have been considered mainly for unsteady non-level flight regimes. Conditions for the ray to turn around and apperance of secondary boom have been derived. Geometrical interpretation and analysis of azimuth ranges for secondary boom propagation have been presented. Evolution of secondary boom ground carpet has been illustrated for unsteady decelerated flight with descent and different headings. Algorithm for disturbances passage through singular turnaround point has been developed. It allows to analyse the ray-tube area distribution and secondary boom signatures. It has been shown that both unsteady and non-level flights provide essential influence on intensity of secondary sonic boom shock waves and their signature shape. So, to obtain reliable computational results, these effects must be taken into account along with imporved prediction of atmospheric attenuation[9] and consideration of non-linear effects in the vicinity of a caustic surface[10].

References

[1] Zhilin Yu.L. Attenuation theory of stationary and non-stationary shock waves in inhomogeneous media. *Trudy TsAGI* , 1094**,** pages 3–13, 1967.

[2] Zhilin Yu.L. Sonic boom from airplane flying along an arbitrary trajectory in stratified atmosphere with three-component wind. *Aeromechanics,* Nauka, Moscow, pages 73–86, 1976.

[3] Hayes W.D., Runyan H.L. Sonic boom propagation through a stratified atmosphere. *J. Acoust. Soc. Am.,* Vol. 51, № 2, Pt. 3, pages 695–701, 1972.

[4] Ivanteyeva L.G.,Chernyshev S.L. About formation of secondary sonic boom carpets. *Trudy TsAGI*, 2670**,** pages 75-90, 2005.

[5] Philippe Blanc-Benon, Laurent Dallois and Julian Scott. Secondary sonic boom modelling for realistic atmospheric conditions. *AIAA Journal (AIAA 2005-2950)*).

[6] Zhilin Yu.L.Conditions for the occurrence of sonic boom focusing. *Uch. Zap. TAGI* , Vol.V, № 2, pages 38–43, 1974.

[7] Hayes W. D. Similarity rules for nonlinear acoustic propagation through a caustic. *Proceedings of Second Conference on Sonic Boom Research*, NASA SP-180, Washington, D.C., pages 165–171, May 1968.

[8] Robinson L.D. Sonic boom propagation through an inhomogeneous, windy atmosphere: Ph.D. dissertation. University of Texas, 118 pages, 1991.

[9] Hugh W. Poling, L. Robinson, Louis C. Sutherland. Supersonic transport secondary sonic booms. *AIAA Journal (AIAA 1997-1659)*.

[10] Auger T., Coulouvrat F. Numerical Simulation of Sonic Boom Focusing. *AIAA Journal,* Vol. 40, № 9, pages 1726–1734, 2002.

This page has been purposedly left blank